11th World Congress on Computational Mechanics (WCCM XI)
5th European Conference on Computational Mechanics (ECCM V)
6th European Conference on Computational Fluid Dynamics (ECFD VI)
E. Oñate, J. Oliver and A. Huerta (Eds)

YIELD DESIGN COMPUTATIONS ON HOMOGENIZED PERIODIC PLATES

JEREMY BLEYER* AND PATRICK DE BUHAN*

* Université Paris-Est, Laboratoire Navier,
Ecole des Ponts ParisTech-IFSTTAR-CNRS (UMR 8205)
6-8 av Blaise Pascal, Cité Descartes, 77455 Champs-sur-Marne, France
e-mail: jeremy.bleyer@enpc.fr, web page: http://navier.enpc.fr/

Key words: Yield design, Limit analysis, Homogenization theory, Thin plates in bending, Yield surface approximation, Finite element method

Abstract. Homogenization approaches have frequently been proposed to evaluate the mechanical properties of highly heterogeneous structures. The determination of such homogenized or macroscopic properties is performed by solving a specific auxiliary problem formulated on an elementary representative volume or a unit cell in the case of periodically heterogeneous materials. Once such properties have been determined, the initial heterogeneous problem is substituted by an equivalent homogeneous one. If global elastic computations using a quite limited number of homogenized moduli are straightforward, this is not the case as regards strength properties. Homogenized yield design or limit analysis computations require, indeed, a semi-analytical description of the homogenized yield surface, simple enough to be efficiently used in an optimization solver.

The following work presents a combined homogenization/approximation approach to perform global computations on periodically heterogeneous thin plates in bending. Homogenization theory in limit analysis or yield design [1, 2] is applied to a thin plate model and macroscopic yield surfaces are derived by solving the auxiliary problem, by means of thin plate finite elements and second-order cone programming.

An original approximation procedure [3] is used to express the so-obtained yield surface as a convex hull of ellipsoids. This simple description enables to formulate yield design problems on a homogenized structure very easily. In particular, a specific attention will be devoted to the formulation of the corresponding static and kinematic approaches as second-order cone programs as well.

An important feature of the method is that upper bound and lower bound status are still preserved on the homogenized problems, so that arising approximation errors can be safely estimated and controlled. Homogenized limit loads can then be bracketed with a

relatively good accuracy. Numerical illustrative applications will be presented on various types of structures like reinforced and perforated plates.

1 INTRODUCTION

Computing ultimate loads on heterogeneous structures can be very difficult to perform, even with competitive numerical methods, due to the high degree of local refinement needed to correctly capture the properties of the inhomogeneities. Homogenization theory in yield design has, therefore, been developed to characterize the strength domain of an equivalent homogeneous medium [1, 2].
Problem (1) represents a yield design problem on a given plate Ω made of a heterogeneous material, the strength properties of which are described by a convex strength criterion G depending on the point $\underline{x} \in \Omega$. The objective is to find the maximal loading factor λ of a reference loading vector $\underline{F}$ such that there exists a bending moment field $\underline{\underline{M}}$ statically admissible (i.e. verifying equilibrium, continuity equations and boundary conditions) with $\lambda\underline{F}$ and satisfying the strength criterion at each point of the plate.

$$\begin{aligned} \lambda_{het} = \max \quad & \lambda \\ \text{s.t.} \quad & \underline{\underline{M}}(\underline{x}) \text{ S.A. with } \lambda\underline{F} \\ & \underline{\underline{M}}(\underline{x}) \in G(\underline{x}) \quad \forall \underline{x} \in \Omega \end{aligned} \tag{1}$$

The principle of the homogenization theory is to replace the previous heterogeneous problem by a similar problem (2) involving an equivalent homogeneous strength criterion G^{hom}, with the idea that this problem would be much easier to solve.

$$\begin{aligned} \lambda_{hom} = \max \quad & \lambda \\ \text{s.t.} \quad & \underline{\underline{M}}(\underline{x}) \text{ S.A. with } \lambda\underline{F} \\ & \underline{\underline{M}}(\underline{x}) \in G^{hom} \quad \forall \underline{x} \in \Omega \end{aligned} \tag{2}$$

In the following, only strength properties $G(\underline{x})$ which vary in a periodic manner throughout the structure will be considered. In this specific case, if a denotes the typical length scale of the heterogeneities and L the typical length of the structure Ω, the main result of homogenization theory states that, under appropriate mathematical assumptions and a proper definition of G^{hom}, $\lambda_{het} \to \lambda_{hom}$ when $a/L \to 0$.

2 DETERMINATION OF THE MACROSCOPIC STRENGTH CRITERION

The macroscopic strength criterion G^{hom} can be computed by solving an auxiliary yield design problem formulated on the unit cell $\mathcal{A}$. Such auxiliary problems are mainly characterized by specific periodic boundary conditions for static and kinematic variables as well as average relations linking microscopic quantities to macroscopic ones. In the case of periodically heterogeneous thin plates in bending, the auxiliary yield design problem

has been formulated in [4]. Let us just recall here the general definition of the macroscopic strength criterion :

$$G^{hom} = \left\{ \underline{\underline{M}} \mid \exists \underline{\underline{m}}(\underline{\xi}) \in SA(\underline{\underline{M}}),\ \forall \underline{\xi} \in \mathcal{A} \quad \underline{\underline{m}}(\underline{\xi}) \in G(\underline{\xi}) \right\} \tag{3}$$

where $\underline{\underline{m}}(\underline{\xi})$ is a microscopic bending moment field defined on the unit cell, $G(\underline{\xi})$ is the local heterogeneous bending strength criterion and where $SA(\underline{\underline{M}})$ denotes the set of microscopic bending moment fields which are statically admissible with a macroscopic bending moment $\underline{\underline{M}}$ i.e. satisfying local equilibrium with zero body forces, continuity equations, periodic boundary conditions and the average relation $\underline{\underline{M}} = \dfrac{1}{|\mathcal{A}|}\displaystyle\int_{\mathcal{A}} \underline{\underline{m}}(\underline{\xi}) dA$. The complete definition of $SA(\underline{\underline{M}})$ can be found in [4].
Besides, by means of the virtual work principle, a dual definition can be given in terms of the macroscopic support function Π_{hom} as follows :

$$\Pi_{hom}(\underline{\underline{\chi}}) = \sup_{\underline{\underline{M}} \in G^{hom}} \underline{\underline{M}} : \underline{\underline{\chi}} = \inf_{v \in KA_0} \frac{1}{|\mathcal{A}|} \left(\int_{\mathcal{A}} \pi(\underline{\underline{\chi}} + \underline{\underline{\underline{\nabla_s \nabla v}}}; \underline{\xi}) dA + \int_{\Gamma} \pi \left(\left[\!\left[\frac{\partial v}{\partial n} \right]\!\right] ; \underline{n} \right) dl \right) \tag{4}$$

where $\underline{\underline{\chi}}$ is the macroscopic virtual curvature, v a periodic fluctuation of the transversal virtual velocity field and π the support function of the heterogeneous local strength criterion $G(\xi)$ computed for the local curvature field $\underline{\underline{\chi}} + \underline{\underline{\underline{\nabla_s \nabla v}}}$ as well as for discontinuities of the normal rotation $[\![\partial v/\partial n]\!]$ through a set of potential yield lines Γ.

Both formulations (3) and (4) are solved numerically using finite element discretization techniques combined with conic programming as proposed in [4]. In particular, it is to be noted that the numerical resolution of (3) yields a subset $G^{stat} \subseteq G^{hom}$ the frontier of which is determined by radial paths along prescribed macroscopic solicitations $\underline{\underline{M}}$. Similarly, the numerical resolution of (4) yields a supset $G^{kin} \supseteq G^{hom}$ the support function of which is sampled for prescribed values of the macroscopic curvature $\underline{\underline{\chi}}$ lying on the three-dimensional unit sphere.

3 APPROXIMATION PROCEDURE

Since G^{stat} and G^{kin} have been numerically determined, it is impossible to solve problem (2) exactly. Besides, in order to keep tractable computations on homogenized structures, it is necessary to obtain a simple semi-analytical description of G^{stat}, G^{kin} with a few parameters only. To this end, an inside approximation $G^{stat}_{app} \subseteq G^{stat} \subseteq G^{hom}$ and an outside approximation $G^{kin}_{app} \supseteq G^{kin} \supseteq G^{hom}$ are constructed and used to solve yield design problems on homogenized structures. Thus, problem (2) will be replaced by the two following yield design problems :

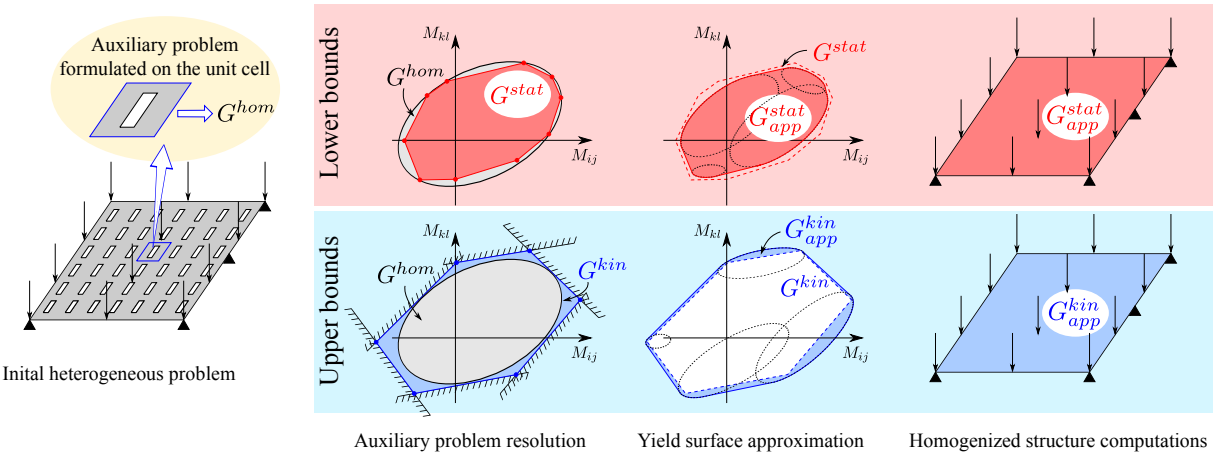

Figure 1: General principle of the combined homogenization/approximation procedure

$$\begin{aligned} \lambda_{lb} = \max \quad & \lambda \\ \text{s.t.} \quad & \underline{\underline{M}}(\underline{x}) \text{ S.A. with } \lambda \underline{F} \\ & \underline{\underline{M}}(\underline{x}) \in G^{stat}_{app} \quad \forall \underline{x} \in \Omega \end{aligned} \tag{5}$$

$$\begin{aligned} \lambda_{ub} = \max \quad & \lambda \\ \text{s.t.} \quad & \underline{\underline{M}}(\underline{x}) \text{ S.A. with } \lambda \underline{F} \\ & \underline{\underline{M}}(\underline{x}) \in G^{kin}_{app} \quad \forall \underline{x} \in \Omega \end{aligned} \tag{6}$$

Due to the inside and outside approximation properties, we have : $\lambda_{lb} \leq \lambda_{hom} \leq \lambda_{ub}$. As a consequence, problem (5) will be used to formulate numerical lower bound static approaches whereas problem (6) will be used for numerical upper bound kinematic approaches as illustrated in Figure 1.

The domain G^{stat}_{app} (resp. G^{kin}_{app}) is obtained by approximating G^{stat} (resp. G^{kin}) by a convex hull of ellipsoids using the procedure described in [3, 5]. The geometrical parameters of the ellipsoids are determined so as to obtain an inside (resp. outside) approximation. Approximating the domain by a convex hull of ellipsoids offers the advantage of a great accuracy with a limited number of parameters. Besides, the corresponding optimization problems can be expressed using second-order cone constraints as shown in the next section.

4 FEM FORMULATIONS OF STATIC AND KINEMATIC APPROACHES

4.1 Expression of the criterion using conic constraints

Let $G = CH(\mathcal{E}_i)$ be a convex hull of n ellipsoids $\mathcal{E}_i \subseteq \mathcal{R}^3$ parametrized by a positive semidefinite upper-triangular matrix $\mathbf{J}_i$ and a vector $\boldsymbol{\mu}_i$ collecting the center coordinates

such that :

$$\mathbf{M}_i \in \mathcal{E}_i \Longleftrightarrow \|{}^T\mathbf{J}_i^{-1}(\mathbf{M}_i - \boldsymbol{\mu}_i)\| \leq 1$$

Using the definition of the convex hull of a finite collection of sets, we have :

$$\mathbf{M} \in G = CH(\mathcal{E}_i) \Longleftrightarrow \exists(\mathbf{M}_i, t_i) \in (\mathbb{R}^3 \times \mathbb{R}^+)^n \text{ such that } \left| \begin{array}{l} \mathbf{M} = \sum_{i=1}^n t_i \mathbf{M}_i \\ \sum_{i=1}^n t_i = 1 \\ \mathbf{M}_i \in \mathcal{E}_i \quad \forall i = 1, \ldots, n \end{array} \right.$$

Using the equation of the ellipsoids and introducing $\tilde{\mathbf{M}}_i = \mathbf{M}_i t_i$ and $\mathbf{r}_i = {}^T\mathbf{J}_i^{-1}(\tilde{\mathbf{M}}_i - t_i\boldsymbol{\mu}_i)$, the criterion can be rewritten :

$$\mathbf{M} \in G = CH(\mathcal{E}_i) \Longleftrightarrow \exists(\mathbf{r}_i, t_i) \in (\mathbb{R}^3 \times \mathbb{R}^+)^n \text{ such that } \left| \begin{array}{l} \mathbf{M} = \sum_{i=1}^n ({}^T\mathbf{J}_i\mathbf{r}_i + t_i\boldsymbol{\mu}_i) \\ \sum_{i=1}^n t_i = 1 \\ \|\mathbf{r}_i\| \leq t_i \quad \forall i = 1, \ldots, n \end{array} \right.$$

It can be observed that $\mathbf{M} \in G$ is now expressed using 4 linear equality constraints and n second-order cone constraints.

For kinematic approaches, the support function of the strength criterion has to be computed. For a convex hull of ellipsoids, the support function $\pi_G(\boldsymbol{\chi})$ is given by :

$$\pi_G(\boldsymbol{\chi}) = \max_{i=1,\ldots,n} \pi_{\mathcal{E}_i}(\boldsymbol{\chi}) = \max_{i=1,\ldots,n} \{\|\mathbf{J}_i\boldsymbol{\chi}\| + {}^T\boldsymbol{\mu}_i \cdot \boldsymbol{\chi}\} \tag{7}$$

4.2 Static approach formulation of the homogenized problem

Equilibrium finite elements are used to solve yield design static approaches on homogenized structures. The plate is discretized by N_E triangular elements assuming a quadratic variation of the bending moment tensor and a linear variation of the shear vector inside each element.
Let $\boldsymbol{\Sigma}$ be the vector of size $24N_E$ collecting all mechanical degrees of freedom (3 components of the bending moment at 3 vertices and 3 mid-nodes and 2 components of the shear force at 3 vertices in one element). All local equilibrium, inter-element continuity equations and boundary conditions are collected in $\mathbf{H}$ and the corresponding load vector is noted $\mathbf{F}$. The strength criterion is verified in each element at N_c checking points (due to the quadratic variation of $\mathbf{M}$ it is not assured to be satisfied in a strict sense, but a sufficient number of checking points (e.g. $N_c = 10$) has proved to be sufficient in practice). Matrix $\mathbf{N}$ is used to express the bending moment at the checking points. The auxiliary

variables are collected in vector $\mathbf{s} = {}^T\langle t_1\,\mathbf{r}_1\ \ldots\ t_p\,\mathbf{r}_p\rangle$ where $p = N_E \times N_c \times n$. The static approach of the homogenized problem can be written as the following second-order cone program:

$$\begin{aligned}\lambda_{lb,h} = \quad & \max \quad \lambda \\ & \text{s.t.} \quad \mathbf{H\Sigma} = \lambda\mathbf{F} \\ & \qquad\ \ \mathbf{N\Sigma} = \mathbf{Ks} \\ & \qquad\ \ \mathbf{Cs} = \mathbf{1} \\ & \qquad\ \ \|\mathbf{r}_i\| \le t_i \quad i = 1,\ldots,p\end{aligned}$$

where $\mathbf{K} = \begin{bmatrix}\tilde{\mathbf{K}} & & \mathbf{0}\\ & \ddots & \\ \mathbf{0} & & \tilde{\mathbf{K}}\end{bmatrix}$, $\tilde{\mathbf{K}} = \begin{bmatrix}\boldsymbol{\mu}_1 & {}^T\mathbf{J}_1 & & \mathbf{0}\\ & \ddots & \ddots & \\ & & \ddots & \ddots \\ \mathbf{0} & & \boldsymbol{\mu}_n & {}^T\mathbf{J}_n\end{bmatrix}$,

$\mathbf{C} = \begin{bmatrix}\overbrace{1\,0\,0\,0\ldots1\,0\,0\,0}^{n\text{ times}} & & \mathbf{0}\\ & \ddots & \\ \mathbf{0} & & \overbrace{1\,0\,0\,0\ldots1\,0\,0\,0}^{n\text{ times}}\end{bmatrix}$.

Provided, if necessary, a post-processing step ensuring that the strength criterion is not violated outside of the checking points, the finite element solution $\lambda_{lb,h}$ of the previous problem is, then, a lower bound of the exact limit load λ_{lb} corresponding to the homogenized yield design problem (5) using a lower bound approximation of G^{hom}.

4.3 Kinematic approach formulation of the homogenized problem

A finite element formulation of the kinematic approach for a strength criterion expressed as a conic hull of ellipsoids has already been presented in [5]. The finite elements are non-conforming cubic triangular elements which authorize inter-element normal rotation discontinuities, so that the maximal resisting work is split into two terms $P_{rm} = P_{rm}^{curv} + P_{rm}^{disc}$ describing, respectively, the contribution of curvature and rotation discontinuities.

The curvature at a given Gauss point in an element can be expressed as $\boldsymbol{\chi}_e = \mathbf{B}_e\mathbf{U}$, so that the contribution of the curvature term to the maximum resisting work is obtained after integration over all Gauss points of the structure :

$$P_{rm}^{curv} = \sum_{e=1}^{q} c_e \max_{i=1,\ldots,n} \{\|\mathbf{J}_i\mathbf{B}_e\mathbf{U}\| + {}^T\boldsymbol{\mu}_i \cdot \mathbf{B}_e\mathbf{U}\}$$

where q is the total number of Gauss points inside the structure and c_e are constant terms coming from the quadrature over the element.

The contribution of inter-element rotation discontinuities to the maximum resisting work, can be written as :

$$P_{rm}^{disc} = \sum_{j=1}^{m} \Pi_{0j} \tilde{c}_j \left| {}^T\boldsymbol{\theta}_j \cdot \mathbf{U} \right|$$

where m is the total number of Gauss points on all edges of the mesh, $\Pi_{0j} = \pi_G(\mathbf{n} \otimes \mathbf{n})$ when $\mathbf{n}$ is the normal vector of the corresponding edge, $\boldsymbol{\theta}_j$ is a vector such that ${}^T\boldsymbol{\theta}_j \cdot \mathbf{U}$ computes the value of the rotation discontinuity through this edge and $\tilde{c}_j$ are constant terms coming from the quadrature over the edge.

Finally, introducing different auxiliary variables, the upper bound kinematic problem can be formulated as :

$$\begin{array}{rlll} \lambda_{ub,h} = & \min & {}^T\mathbf{c} \cdot \mathbf{y} + {}^T\mathbf{c}' \cdot \mathbf{s} & \\ & \text{s.t.} & {}^T\mathbf{F} \cdot \mathbf{U} = 1 & \\ & & \mathbf{r} = \mathbf{L}\mathbf{U} & \\ & & \|\mathbf{r}_j\| \leq t_j & j = 1, ..., n \times q \\ & & \mathbf{w}_e + \mathbf{P}\mathbf{B}_e\mathbf{U} \leq y_e & e = 1, ..., q \\ & & \mathbf{u} = \boldsymbol{\Theta}\mathbf{U} & \\ & & |\mathbf{u}| \leq \mathbf{s} & \end{array} \tag{8}$$

where $\mathbf{L} = \begin{bmatrix} \tilde{\mathbf{L}}\mathbf{B}_1 & & \mathbf{0} \\ & \ddots & \\ \mathbf{0} & & \tilde{\mathbf{L}}\mathbf{B}_q \end{bmatrix}$, $\tilde{\mathbf{L}} = \begin{bmatrix} \mathbf{J}_1 & & \mathbf{0} \\ & \ddots & \\ \mathbf{0} & & \mathbf{J}_n \end{bmatrix}$, $\mathbf{P} = \begin{bmatrix} {}^T\boldsymbol{\mu}_1 & & \mathbf{0} \\ & \ddots & \\ \mathbf{0} & & {}^T\boldsymbol{\mu}_n \end{bmatrix}$, $\mathbf{t} = {}^T\langle \mathbf{w}_1 \dots \mathbf{w}_q \rangle$,

$\boldsymbol{\Theta} = \begin{bmatrix} {}^T\boldsymbol{\theta}_1 \\ \vdots \\ {}^T\boldsymbol{\theta}_m \end{bmatrix}$ and ${}^T\mathbf{c}' = \langle \Pi_{01}\tilde{c}_1 \ \dots \ \Pi_{0m}\tilde{c}_m \rangle$.

This is a also a standard SOCP problem, the solution of which provides an upper bound $\lambda_{ub,h}$ of the exact limit load λ_{ub} corresponding to the homogenized yield design problem (6) using an upper bound approximation of G^{hom}.

5 A priori error estimation

As the proposed homogenization/approximation procedure involves different approximation steps, it is useful to obtain an estimate of the final error made on the exact limit load λ_{hom}.

Hence, the following different errors are defined :

- ϵ_0 denotes the error made when solving discrete auxiliary problems. It is estimated by measuring the relative distance between the sets G^{stat} and G^{kin} :

$$\epsilon_0 = \frac{d_H(G^{stat}, G^{kin})}{\|\pi_{G^{stat}}\|_\infty}$$

where $\|\cdot\|_\infty$ is the max-norm on the unit sphere and $d_H(\cdot,\cdot)$ is the Hausdorff distance.[1]

- $\epsilon^s_{(n)}$ denotes the error made when approximating G^{stat} from the inside by a convex hull of n ellipsoids. It is estimated similarly as before :

$$\epsilon^s_{(n)} = \frac{d_H(G^{stat}, G^{stat}_{app})}{\|\pi_{G^{stat}}\|_\infty}$$

- $\epsilon^k_{(n)}$ denotes the error made when approximating G^{kin} from the outside by a convex hull of n ellipsoids :

$$\epsilon^k_{(n)} = \frac{d_H(G^{kin}, G^{kin}_{app})}{\|\pi_{G^{kin}}\|_\infty}$$

The exact limit load λ_{hom} obtained with G^{hom} can then be bracketed by the following estimation :

$$(1-\epsilon_0-\epsilon^s_{(n)})\lambda_{hom} \leq \lambda_{lb} \leq \lambda_{hom} \leq \lambda_{ub} \leq (1+\epsilon_0+\epsilon^k_{(n)})\lambda_{hom}$$

One has also to take into account the error made by the finite element approximations when solving the homogenized problems introducing a new error ϵ^s_h and ϵ^k_h which depend on the mesh size used by both approaches. Finally, the relative gap between the computed lower and upper bound can be estimated by :

$$\frac{\lambda_{ub,h}-\lambda_{lb,h}}{\lambda_{hom}} \leq \delta = \epsilon_0 + \epsilon^s_{(n)} + \epsilon^k_{(n)} + \epsilon^s_h + \epsilon^k_h$$

6 ILLUSTRATIVE APPLICATIONS

6.1 Reinforced rectangular plates

The first example is concerned with plates consisting of a matrix obeying the von Mises criterion with an ultimate bending moment $m_{p1} = 1$ reinforced by a straight band of reinforcing material obeying the same criterion with an ultimate bending moment $m_{p2} = 40$. The relative area of the reinforcing material is fixed to 5%. The unit cell, along with the mesh used to solve the auxiliary problem, is represented in Figure 2(a). The error made when solving discrete auxiliary problems has been estimated to $\epsilon_0 = 2.22\%$. Both domains G^{stat} and G^{kin} have then been approximated using a convex hull of $n = 10, 30$ and 50 ellipsoids, the corresponding errors are given in Table 1.

Four different yield design problems have been considered : a square plate of side length $a = b = 1$ and a rectangular plate of side lengths $a = 1, b = 1.5$ are subjected

[1] The Hausdorff distance between two convex sets A and B can be defined using their support functions as $d_H(A,B) = \max_{d\in\mathbb{S}} |\pi_A(d) - \pi_B(d)| = \|\pi_A - \pi_B\|_\infty$.

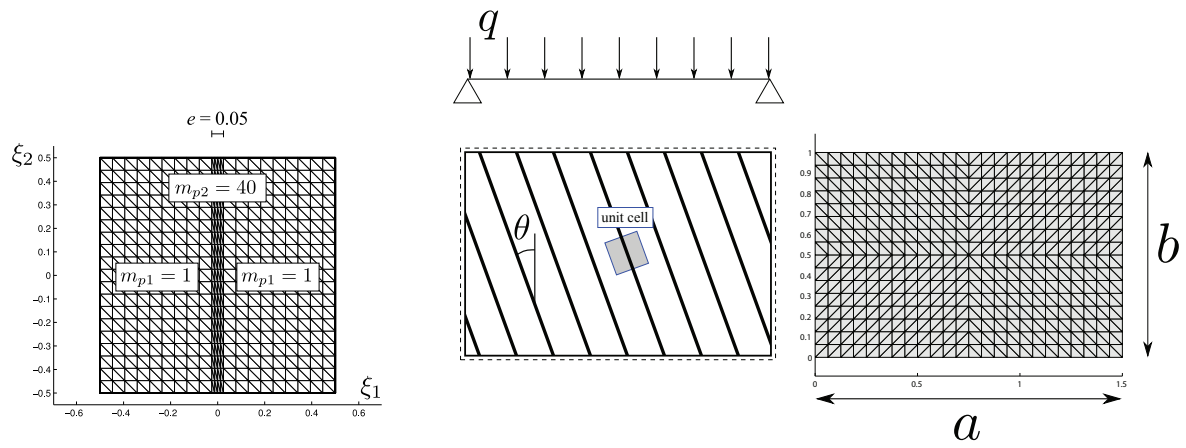

(a) The unit cell and its mesh

(b) The rectangular plate problem

Figure 2: A reinforced plate problem

Errors	$\epsilon^s_{(n)}$	$\epsilon^k_{(n)}$
10 ell.	17.43%	17.99%
30 ell.	5.20%	4.51%
50 ell.	3.09%	2.45%

Table 1: Table of errors induced by the approximation

to a uniformly distributed pressure q. The plate edges are, in both cases, either simply supported or fully clamped. The limit load q is estimated, for the four problems, for different values of the reinforcement orientation angle θ with respect to the plate smallest edge direction (see Figure 2(b)). The limit load obtained for an unreinforced plate is denoted by q_0.

The error induced by the finite element discretization on the global structure computation has been estimated by solving simply supported and clamped problems on the different geometries with a homogeneous von Mises criterion. It has been found that $\epsilon^s_h + \epsilon^k_h \approx 0.3\%$ for simply supported problems and $\epsilon^s_h + \epsilon^k_h \approx 1.3\%$ for clamped problems for both geometries. Finally, for 50 ellipsoids, the following estimates of the relative gap δ have been obtained :

- $\delta \approx 8\%$ for simply supported problems
- $\delta \approx 9\%$ for clamped problems

Figures 3 and 4 represent the obtained lower and upper bound estimates of $\lambda^{hom} = q/q_0$ for the different problems, varying reinforcement orientations and different degrees of approximation. The gray zone represents the estimated relative gap zone of width δ and centered on the average between the best lower bound and upper bound estimates. The Reuss lower bound ($q = q_0$) obtained when replacing the heterogeneous material by the

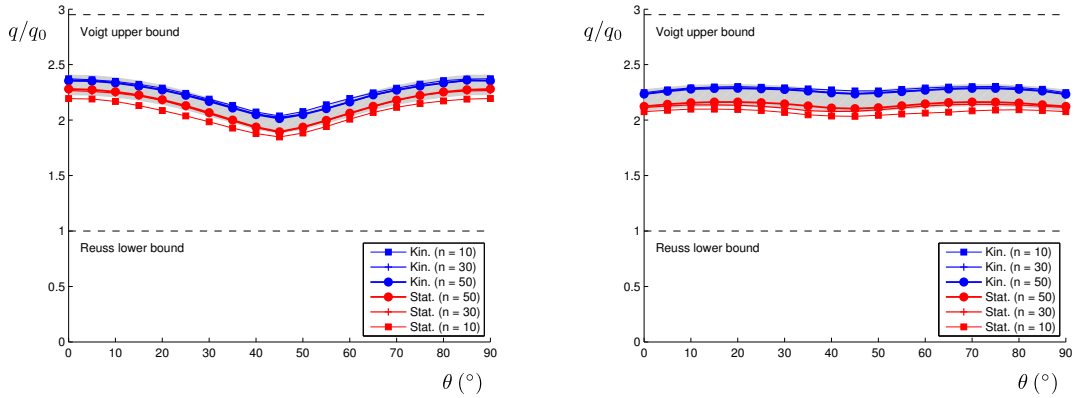

(a) Simple supports (b) Clamped supports

Figure 3: Square plate ($a = b = 1$) problems

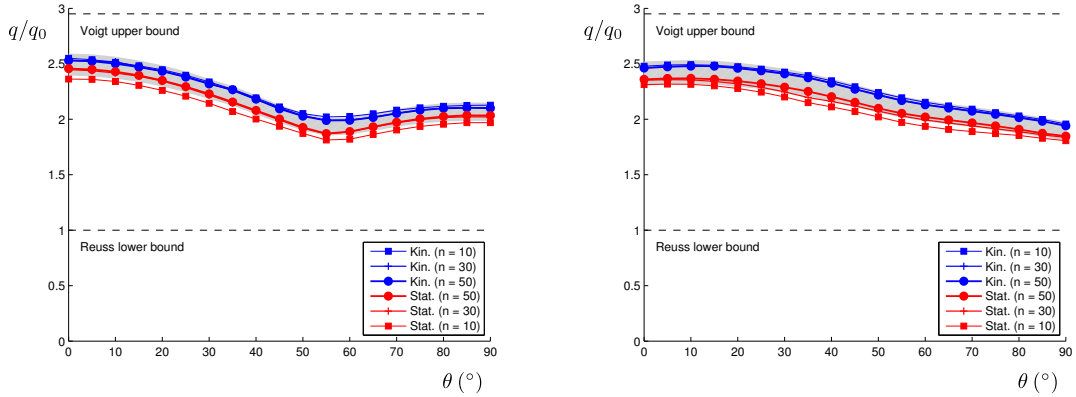

(a) Simple supports (b) Clamped supports

Figure 4: Rectangular plate ($a = 1, b = 1.5$) problems

weakest material and the Voigt upper bound ($q = \langle m_p \rangle q_0$) obtained by using the average of the ultimate bending moment are represented for information.
One can observe that the lower and upper bounds are very close from each other and that the best estimates obtained with 50 ellipsoids fall within the estimated relative gap zone. Despite the anisotropy of the considered problem, the accuracy of the obtained bounds do not seem to depend on this anisotropy.

6.2 Slotted circular plate

The second example concerns a circular plate perforated by elongated holes with round edges disposed in staggered rows, a pattern frequently encountered in perforated metal sheets (Figure 5(a)). The porosity is $\eta = 0.26$. The plate is loaded by a uniformly distributed pressure and is simply supported. Due to the pattern symmetry, only a

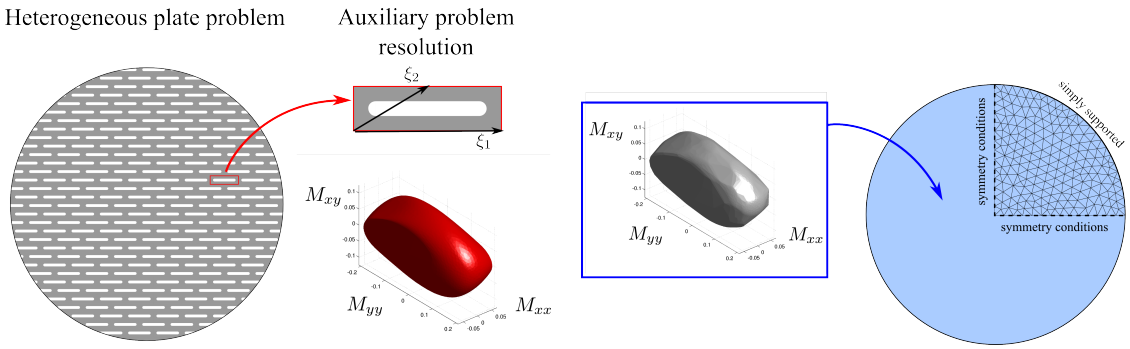

(a) Heterogeneous problem, unit cell and macroscopic strength criterion

(b) Approximated criterion and homogenized problem

Figure 5: Homogenization/approximation procedure for the slotted circular plate problem

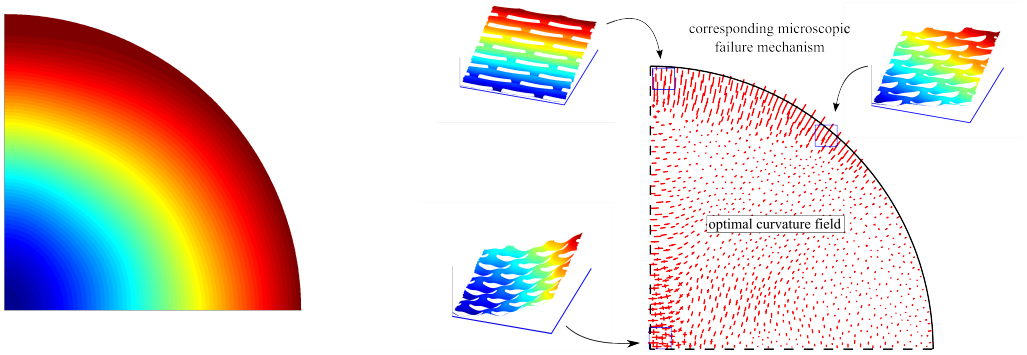

(a) Optimal velocity field (red corresponds to zero values and blue to the highest ones)

(b) Principal directions of the curvature field and associated microscopic collapse mechanisms

Figure 6: Optimal kinematic fields for the slotted circular plate problem

quarter of the plate has been modeled in the homogenized computation (Figure 5(b)).

As before, the macroscopic strength criterion has been approximated using up to 50 ellipsoids (see Figure 5(b) for the approximating surface). The ultimate pressure q normalized by the one obtained for a non-perforated plate times the porosity ηq_0 has been bracketed as : $0.496 \leq q/\eta q_0 \leq 0.511$.

Finally, the optimal transversal velocity field obtained by the kinematic approach has been represented in Figure 6(a). The principal directions of the associated curvature field have been represented in Figure 6(b). One can clearly observe the anisotropy induced by the hole pattern since the solution is no more axisymmetric. Besides, it is also possible to plot the microscopic collapse mechanisms of the unit cell corresponding to a particular value of the curvature at a given region of the plate. For clarity, the periodic fluctuations have been magnified compared to the global curvature strain. One can observe that the collapse mechanisms are quite different with respect to the corresponding macroscopic curvatures.

7 Conclusion

A combined homogenization/approximation method has been proposed for evaluating ultimate loads on periodically heterogeneous structures using the tools of yield design or limit analysis theory. Starting from the formulation of an auxiliary yield design problem on the unit cell, numerical estimates of the macroscopic yield surface are computed from a finite element resolution of the corresponding static and kinematic approaches. Semi-analytical approximations of such surfaces using a convex hull of ellipsoids are then derived to obtain a simple and accurate mathematical description using conic constraints. These surfaces are then used in the finite element computation at the macroscopic level on the homogenized structure, the corresponding optimization problems being formulated as second-order cone programs.
One specific aspect of the approach is that, at each step of the procedure, a specific attention is devoted to the conservation of the bounding status of the different computations, the yield surfaces used in the static (resp. kinematic) approach being always lower (resp. upper) bound approximations of the exact one. This enables to keep the bounding status on the macroscopic computation. It is even possible to obtain very good estimates of the relative gap between the corresponding lower and upper bound estimates of the homogenized ultimate load.
This method has been illustrated on periodic heterogeneous thin plates in bending but the general principle can be applied to any mechanical model, although the main bottleneck will probably be the dimension of the considered yield surfaces (e.g. dimension 6 for anisotropic 3D continua).

REFERENCES

[1] P. Suquet. Elements of homogenization of inelastic solid mechanics, *Homogenization techniques for composite media*, Vol. **272**, 193–278, 1985.

[2] P. de Buhan. A fundamental approach to the yield design of reinforced soil structures, *Ph.D. thesis, Thèse d'Etat*, Paris VI, 1986.

[3] J. Bleyer, P. de Buhan. A greedy algorithm for yield surface approximation, *Comptes Rendus Mécanique*. Vol. **341**, 605–615, 2013.

[4] J. Bleyer, P. de Buhan. A computational homogenization approach for the yield design of periodic thin plates - Part I : Construction of the macroscopic strength criterion. *International Journal of Solids and Structures*, (accepted) , 2014.

[5] J. Bleyer, P. de Buhan. A computational homogenization approach for the yield design of periodic thin plates - Part II : Upper bound yield design calculation of the homogenized structure. *International Journal of Solids and Structures*, (accepted) , 2014.